

Interpolating atmospheric water vapor delay by incorporating terrain elevation information

W. B. Xu · Z. W. Li · X. L. Ding · J. J. Zhu

Received: 18 August 2010 / Accepted: 22 February 2011 / Published online: 8 March 2011
© Springer-Verlag 2011

Abstract In radio signal-based observing systems, such as Global Positioning System (GPS) and Interferometric Synthetic Aperture Radar (InSAR), the water vapor in the atmosphere will cause delays during the signal transmission. Such delays vary significantly with terrain elevation. In the case when atmospheric delays are to be eliminated from the measured raw signals, spatial interpolators may be needed. By taking advantage of available terrain elevation information during spatial interpolation process, the accuracy of the atmospheric delay mapping can be considerably improved. This paper first reviews three elevation-dependent water vapor interpolation models, i.e., the Best Linear Unbiased Estimator in combination with the water vapor Height Scaling Model (BLUE+HSM), the Best Linear Unbiased Estimator coupled with the Elevation-dependent Covariance Model (BLUE+ECM), and the Simple Kriging with varying local means based on the Baby semi-empirical model (SKlm+Baby for short). A revision to the SKlm+Baby model is then presented, where the Onn water vapor delay model is adopted to substitute the inaccurate Baby semi-empirical model (SKlm+Onn for short). Experiments with the zenith wet delays obtained through the GPS observations from the Southern California Integrated GPS Network (SCIGN) demonstrate that the SKlm+Onn model outperforms the other three. The RMS of SKlm+Onn is only 0.55 cm, while those of BLUE+HSM, BLUE+ECM and

SKlm+Baby amount to 1.11, 1.49 and 0.77 cm, respectively. The proposed SKlm+Onn model therefore represents an improvement of 29–63% over the other known models.

Keywords Water vapor delay · Interpolation model · GPS

1 Introduction

When radio signals such as those of Global Positioning System (GPS) and Synthetic Aperture Radar (SAR) travel through the atmosphere, they will suffer from propagation delays due to atmospheric refraction. The hydrostatic component of the atmospheric delay, primarily due to dry gases in the troposphere, can be fairly accurately estimated using surface atmospheric pressure measurements. Such delays can reach up to 2.3 m in the zenith direction. However, the wet component of the atmospheric delay, up to a few decimeters in magnitude, is difficult to be accurately modeled due to the lack of means to map the dynamic structure of the moisture field with sufficient temporal and spatial resolutions. With the advent of GPS technology, the delays caused by water vapor can be measured very accurately at high temporal resolution. In the applications where atmospheric effects need to be eliminated, such as, interferometric synthetic aperture radar (InSAR), the tropospheric zenith delays derived from GPS measurements can significantly contribute to the elimination processing in terms of calibration (Dodson et al. 1996; Li et al. 2007). However, the spatial distribution of continuously operated GPS stations is often quite poor. Thus, an efficient spatial interpolation model of water vapor is of great interest (Williams et al. 1998).

New methods have recently been introduced in the GPS-related literature for interpolating water vapor data using GPS observations at relatively isolated stations.

W. B. Xu · Z. W. Li (✉) · X. L. Ding · J. J. Zhu
School of Geosciences and Info-Physics,
Central South University,
Changsha 410083, Hunan, China
e-mail: zwli@mail.csu.edu.cn

X. L. Ding
Department of Land Surveying and Geo-Informatics,
The Hong Kong Polytechnic University,
Hung Hom, Kowloon, Hong Kong, China

Jarlemark and Emardson (1998) presented three different strategies, i.e., the gradient method, the turbulence method and the linear regression in time, to interpolate the wet tropospheric delays. Among them, the turbulence method has less root mean square (RMS) errors than the other two. Janssen et al. (2004) discussed the applications of Inverse Distance Weighted (IDW), Ordinary Kriging (OK) and spline interpolation methods for GPS zenith wet delays interpolation and concluded that IDW and OK are better than spline interpolation. Janssen et al. (2004) also demonstrated the practical use of the models in potential InSAR atmospheric correction. However, all these models do not consider the terrain elevation dependence of water vapor. As a result, the interpolation outcome may contain large errors in the regions where the topography is highly varying.

The first elevation-dependent water vapor interpolation method was given by Emardson and Johansson (1998). They propose to: (1) use a Height Scaling Model (HSM) to scale the water vapor data of different sites to a uniform height; (2) perform interpolation with the scaled water vapor using the Best Linear Unbiased Estimator (BLUE); (3) scale the interpolated water vapor back to its original height. We shall use BLUE+HSM to abbreviate it hereinafter. This model has been assessed by cross-validation analysis and its accuracy is found to be about 1 cm. However, it should be noted that the maximal height difference in the studied case is only 214 m and its performance in areas of highly varying topography has not yet been reported. More recently, Li et al. (2006b) proposed an elevation-dependent GPS water vapor model, also based on the BLUE method. That model differs from the previous model by employing an Elevation-dependent Covariance Model to determine the BLUE weights. For simplicity, we call it BLUE+ECM (i.e., Elevation-dependent Covariance Model). However, the model needs a large number of GPS water vapor measurements to establish a reliable elevation-dependent variance/covariance function, which limits the practical use of the model. Li et al. (2006a) proposed another elevation-dependent atmospheric water vapor interpolation model based on the estimator of Simple Kriging with varying local means (SKlm), which is a geostatistical method that can incorporate secondary information such as elevation, and the Baby tropospheric semi-empirical model (Baby et al. 1988), which is used to model the varying local means in SKlm. For convenience, we will call it SKlm+Baby hereinafter. Compared to BLUE+ECM, this model does not need any GPS water vapor measurements and can be easily implemented. However, it does need ground meteorological data at a reference station.

In this paper, we will present a modified version of the SKlm+Baby model, by substituting the Baby semi-empirical model with the Onn model, which is an exponential law model of water vapor with the elevation as adopted by Onn and Zebker (2006). What motivates us to do this is that

the Baby semi-empirical model assumes the relative humidity remains constant up to a certain height while the water vapor actually has great variability at different heights. This may lead to errors in modeling the varying local means in SKlm. The Onn model can better model the varying local means, thus improves the accuracy of the SKlm model. A comprehensive comparison among SKlm+Onn and the previous three elevation-dependent water vapor models will be presented in the following sections.

The paper is organized as follows. In Sect. 2, three existing elevation-dependent water vapor models, i.e., BLUE+HSM, BLUE+ECM and SKlm+Baby, are reviewed, followed by the modification of SKlm+Baby in Sect. 3. The different elevation-dependent models are compared in Sect. 4.

2 Existing elevation-dependent water vapor models

2.1 BLUE+Height Scaling Model

The zenith wet delay at a given location can be estimated by a linear estimator

$$Z^*(u) = \sum_{i=1}^n w_i \cdot Z(u_i), \quad (1)$$

where $Z(u_i)$ denotes the measured zenith wet delay at location u_i , and w_i is the weight of $Z(u_i)$ which will be determined through different optimization rules.

By minimizing the mean square differences between the estimated and the true zenith wet delays, the BLUE estimator of zenith wet delays can be constructed, whose weights can be expressed in vector form (Emardson and Johansson 1998):

$$w_{\text{BLUE}} = C_{m,m}^{-1} \cdot C_{m,e} + \frac{(1 - C_{m,e}^T \cdot C_{m,m}^{-1} \cdot s) \cdot C_{m,m}^{-1} \cdot s}{s^T \cdot C_{m,m}^{-1} \cdot s}, \quad (2)$$

where $C_{m,m}$ is the covariance matrix between measured zenith wet delays, $C_{m,e}$ is the covariance matrix between the measured and the estimated (interpolated) zenith wet delays, and s is a unit vector, with its size equal to the number of measured zenith wet delays.

The covariance of zenith wet delays at two locations separated by L can be estimated by (Emardson and Johansson 1998)

$$C(L) = \sigma^2 - \frac{1}{2} c L^n, \quad (3)$$

where σ^2 is the variance of the zenith wet delays, c and n are constants of water vapor turbulence (Treuhhaft and Lanyi 1987), with $c = 4.5 \times 10^{-5} \text{ cm}^2/\text{m}$, $n = 1$ and $\sigma^2 = 20 \text{ cm}^2$ as quoted from Emardson et al. (1998). These constants are

optimized mainly for Sweden area and need to be adjusted when applied to other areas.

Equations (1) and (2) form the BLUE estimator of zenith wet delays. The estimator does not consider the elevation-dependent nature of water vapor. To account for this, [Emardson and Johansson \(1998\)](#) suggest scaling the zenith wet delays from nearby sites (i.e., elevations) into a reference elevation prior to the BLUE interpolation based on [Elosegui et al. \(1998\)](#)

$$Z_{\text{ref}}(u) = Z(u) \cdot e^{(h-h_{\text{ref}})/H}, \quad (4)$$

where $Z(u)$ is the measured zenith wet delay at height h , $Z_{\text{ref}}(u)$ is the zenith wet delay scaled to the reference height h_{ref} , and H is the averaged water vapor scale height that is usually 1–2 km.

After the BLUE estimation, the interpolated zenith wet delay is then scaled back to its original height h with the inversion of Eq. (4). Cross-validation results show that the model can reach an interpolation accuracy of about 1 cm, even with a sparse GPS network ([Emardson and Johansson 1998](#)). However, as noted earlier, the maximal height difference between the GPS stations in the network is only 214 m. Therefore, its performance over the areas with greater varying topography should be checked.

2.2 BLUE + Elevation-dependent Covariance Model

This model was originally designed to interpolate the differential water vapor delays between SAR acquisitions in order to correct the tropospheric effects in InSAR ([Li et al. 2006b](#)). The model is generally known as GPS Topography-dependent Turbulence Model (GTTM).

This model also uses the BLUE estimator where the covariance function adopted to derive the BLUE weights is ([Li et al. 2006b](#))

$$C(L) = C(0) - \frac{1}{2}D(L), \quad (5)$$

where $D(L)$ is the structure function of zenith wet delays. $D(L)$ may be calculated from the variance of water vapor delays σ_{int} in a SAR interferogram when the two SAR acquisitions are sufficiently separated in time (e.g., longer than 1 day)

$$D(L) = \frac{1}{2}\sigma_{\text{int}}^2 \quad (6)$$

with

$$\sigma_{\text{int}} = kH + cL^n, \quad (7)$$

where L and H are, respectively, the distance and the height differences in km between any two locations considered, c , n and k are empirical constants that may be estimated from available datasets. For example, using GPS water vapor

measurements at 126 stations over the Southern California Integrated GPS Network (SCIGN) and during the period of January 1998 to March 2000, [Emardson et al. \(2003\)](#) simulated the potential effects of water vapor delays in interferometric measurements and found that $c = 2.8$, $n = 0.44$, and $k = 0.5$ for observation intervals of 1 day.

2.3 SKlm+Baby semi-empirical model

The basic equation of SKlm is ([Goovaerts 1997; Li et al. 2006a](#))

$$Z_{\text{SKlm}}^*(u) = \sum_{i=1}^n w_i^{\text{SK}} [Z(u_i) - m_{\text{SK}}^*(u_i)] + m_{\text{SK}}^*(u), \quad (8)$$

where $Z_{\text{SKlm}}^*(u)$ is the interpolated zenith wet delay at location u , $Z(u_i)$ is the measured zenith wet delay at location u_i , n is the number of measured water vapor delays used for the interpolation, w_i^{SK} are the kriging weights to be determined, $m_{\text{SK}}^*(u_i)$ and $m_{\text{SK}}^*(u)$ are the varying local means at locations u_i and u , respectively. The varying local means are used to distinguish the stationary means in geostatistics. They are calculated through their correlations with other variables (e.g. elevations) that may be easily obtained ([Goovaerts 1997](#)). Here, the varying local means (i.e. zenith wet delays) are calculated through terrain elevations. The relationship between zenith wet delay and terrain elevation will be discussed below.

In the scheme of SKlm+Baby, the Baby semi-empirical model ([Baby et al. 1988](#)) is used to model the varying local means, i.e., the elevation-dependent component of the atmospheric delay by ([Li et al. 2006a](#))

$$m_{\text{SK}}^*(u) = 0.0022768P_h + vU_h 10^{\gamma T_h}, \quad (9)$$

where v and γ are site- and season-specific constants, respectively. The atmospheric pressure P_h , temperature T_h , and relative humidity U_h are calculated by their vertical gradient models:

$$P_h = P_0(1 - 22.6 \times 10^{-6}(h(u) - h_0))^{5.26} \quad (10)$$

$$T_h = T_0 - k(h(u) - h_0) \quad (11)$$

$$U_h = U_0, \quad (12)$$

where P_0 , T_0 and U_0 are meteorological observations at a reference station, k is the temperature elapse constant, h_0 is the elevation of the reference station, and $h(u)$ is the elevation of location u . The first term in Eq. (9), which depends on atmospheric pressure, is known as the hydrostatic component while the second term, which depends on temperature and relative humidity, is known as the wet component. As this paper discusses only the interpolation of zenith wet delays,

the first term in Eq. (9) should be excluded and thus it reduces to

$$m_{SK}^*(u) = vU_h 10^{\gamma T_h} \quad (13)$$

The kriging weights w_i^{SK} in Eq. (8) can be obtained by solving the following system

$$\sum_{i=1}^n w_i^{SK} C_R(u_i - u_j) = C_R(u_i - u), \quad j = 1, \dots, n, \quad (14)$$

where C_R is the covariance function of the residual water vapor delays $R(u) = Z(u) - m_{SK}^*(u)$. $C_R(u_i - u_j)$ can be estimated by (Li et al. 2006a)

$$C_R(u_i - u_j) = \gamma_R(\infty) - \gamma_R(d), \quad (15)$$

where $d = u_i - u_j$ and $\gamma_R(d)$ is the semivariogram (as a half structure function) model of residual water vapor delays that can be fitted with available datasets. Li et al. (2006a) proposed a power law model for $\gamma_R(d)$, i.e., $\gamma_R(d) = g_0 + Cd^{3/5}$, based on the fact that water vapor turbulence follows a power law. This makes $\gamma_R(d)$ not converge at infinity. It is physically implausible and must be flattened beyond some saturation length. Following Treuhaft and Lanyi (1987), Li et al. (2006a) take a saturation length of 3,000 km.

3 Revision of the SKlm + Baby semi-empirical model

The accuracy of SKlm is strongly dependent on the accuracy of the varying local means. The SKlm + Baby interpolator uses the Baby semi-empirical model, the meteorological data at a reference station and the vertical gradient models of atmospheric pressure, temperature and relative humidity to model the varying local means, i.e., the elevation-dependent component of water vapor delay. As the meteorological data at a sole reference station is used and the Baby semi-empirical model itself has an uncertainty up to several centimeters (Li et al. 2008), the elevation-dependent component of water vapor delay is difficult to be modeled accurately with SKlm + Baby (see Sect. 4.2). We therefore propose to use a more straightforward elevation-related regression function (Onn and Zebker 2006) to model the elevation-dependent component of water vapor delay,

$$Z^*(h) = m_{SK}^*(u_i) = Ce^{-\alpha h} + h\alpha Ce^{-\alpha h} + Z_{\min}, \quad (16)$$

where $Z^*(h)$ is the regressed zenith wet delay at height h , C is proportional to the amount of zenith wet delay measured at sea level, α is the delay rate of the vertical water vapor profile, and Z_{\min} is the zenith wet delay value at the highest location. C , α and Z_{\min} can be estimated by regression analysis.

The difference between this revised model and SKlm + Baby lies in the way of modeling the varying local means (namely the elevation-dependent component of wet delay), i.e., the Onn model for the former and the Baby model for the latter. The implementation of the revised model is as follows: (1) determining the elevation-dependent model of zenith wet delays (Eq. 16) through regression analysis, (2) calculating the varying local means based on the regression model and the covariances of residual wet delays based on Eq. (15) and (3) determining the Kriging weights by Eq. (14) and then calculating the interpolated zenith wet delays through Eq. (8). As the revised model is the integration of SKlm and Onn model, we called it SKlm + Onn hereinafter.

4 Model evaluation

4.1 Data

SCIGN is one of the densest GPS networks worldwide, with more than 250 continuously operated GPS stations. The received GPS data can be freely downloaded and have been analyzed by well-established research facilities such as Scripps Orbit and Permanent Array Center (SOPAC), University of California San Diego (UCSD), Jet Propulsion Laboratory (JPL), and many others. In addition, Southern California is a tectonic active region. The calibration of zenith wet delays for geodetic measurements like InSAR in this region is of great scientific interest. 120 GPS stations of the SCIGN network operating over the greater Los Angeles metropolitan area will be used in this study. Their distribution is illustrated in Fig. 1. The data recorded at the GPS stations have been analyzed by the SOPAC, where the daily three-dimensional position data series and hourly GPS total zenith delays at each SCIGN site are routinely produced (<http://sopac.ucsd.edu>). The hydrostatic delays at each SCIGN site are estimated using surface meteorological data and then subtracted from the total zenith delays to generate the zenith wet delays (Liu 2000). We will use these zenith wet delay measurements to evaluate the interpolators discussed above in Sects. 2 and 3. Considering that one of the main goals of developing water vapor interpolation models is to mitigate water vapor effects on InSAR, we first choose the zenith wet delay measurements at 18:00 UTC on 25 May, 3 August and 12 October 2002, which are only half an hour earlier than the ERS-2 SAR acquisitions, to conduct detailed interpolation comparisons among the interpolators in Sect. 4.2. Then we use 6 months' zenith wet delay measurements, spanning from 1 May to 31 October, 2002, to evaluate the accuracy of the interpolators in Sect. 4.3.

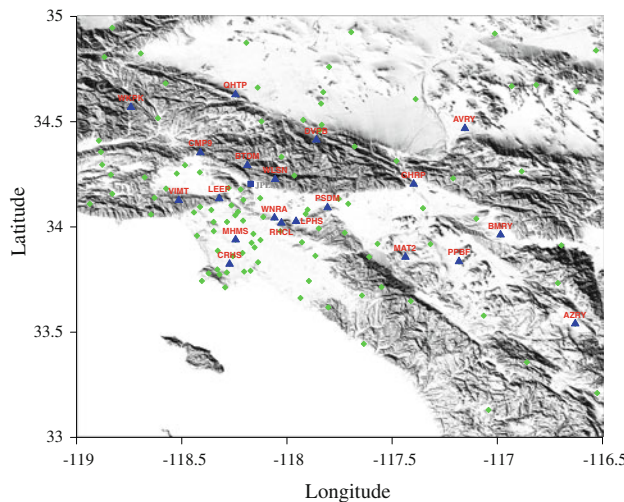


Fig. 1 Distribution of SCIGN GPS stations used in this study, as superposed on the Shuttle Radar Topography Mission (SRTM) DEM. Zenith wet delay measurements at the GPS stations indicated by blue triangles will be used as “validation samples” for the cross-validation analysis in Sects. 4.2 and 4.3. Meteorological data at station JPLM marked by a blue square will be used as reference data for the BLUE + HSM and the SKlm + Baby interpolators

4.2 Detailed interpolation comparisons at three epochs

4.2.1 Elevation-dependent component of zenith wet delay

The accuracy of an elevation-dependent water vapor model depends primarily on the modeling accuracy of the elevation-dependent component of zenith wet delays. The four elevation-dependent models use different strategies to model this component. We will in this section compare the performances of the models in determining the elevation-dependent component of zenith wet delays. As the BLUE+ECM interpolator models the elevation-dependent component as part of the covariance modeling, this model will not be included in this comparison. Figure 2 shows the elevation-dependent components of the zenith wet delays from the BLUE+HSM, the SKlm+Baby and the SKlm+Onn interpolators, as calculated from the inversion of Eqs. (4), (13) and (16). In the calculations, GPS zenith wet delay measurements and meteorological data at station JPLM are used as reference data for the Height Scaling Model and the Baby semi-empirical model. The station JPLM is chosen because it has simultaneously recorded meteorological data, and is located nearly in the center of the network with moderate altitude, and without any data gaps. The parameters in the Onn model are determined by regression from the available GPS zenith wet delay samples.

It is obvious that in all the subplots of Fig. 2 the zenith wet delays are negatively correlated with elevation. The Onn model fits the observation samples best, followed by the Height Scaling Model, while the Baby semi-empirical model

shows significant systematic deviations from the observation samples. These systematic differences can be explained by the fact that the Onn model is regressed from the observations at all available GPS stations, while the Height Scaling Model and the Baby semi-empirical model are only referenced to the observations at station JPLM.

4.2.2 Semivariogram

A semivariogram of atmospheric water vapor reflects the spatial variability characteristics of the water vapor distribution. It is crucial to build accurate individual semivariograms for the four elevation-dependent interpolators in order to construct the covariance model required in the models. Assuming that the spatial water vapor field is homogeneous, isotropic and ergodic, we calculate the semivariogram models of the GPS zenith wet delays, and the de-trended GPS zenith wet delays (i.e., after removing the elevation-dependent components) by the Baby and the Onn models for epoch 18:00 UTC of 25 May, 3 August and 12 October 2002, respectively. Figure 3 shows the calculated semivariograms, where the left column gives the models calculated from the GPS zenith wet delays while the middle and right columns give the models calculated from the de-trended GPS zenith wet delays by the Baby semi-empirical model and the Onn model. The first to the third rows of Fig. 3 correspond to the dates of 25 May, 3 August and 12 October 2002, respectively. Please note that the scales of Y axis are different among the three columns in Fig. 3. This spatial variability analysis shows that the semivariograms (a), (c), (d), (g) and (i) in Fig. 3 follow the spherical model while the rest are in the power law model. By incorporating these half structure functions with Eq. (15), the covariance of residual zenith wet delays can be constructed. Since the power law model does not converge at infinity, it needs to be flattened with a saturation length as discussed in Sect. 2.3.

4.2.3 Comparison of the interpolation results

The method of cross validation is adopted to evaluate the performances of the four interpolators at the three chosen epochs. For each epoch, the GPS zenith wet delay measurements at 20 GPS stations (c.f. Figs. 1 and 4 for those GPS stations) are removed from the dataset, and the zenith wet delays from the other stations are used to interpolate the zenith wet delays at the removed (validation) stations. The maximum and minimum altitudes of the total 120 GPS stations are 2,227.2 and −28.5 m, while those of the 20 GPS stations used for validation are 1,705.3 and −23.5 m, respectively. Of all the 120 GPS stations, six are located above 1,705.3 m and three below −23.5 m. In the interpolation, the covariances of zenith wet delays utilized in the BLUE+HSM, the SKlm+Baby and the SKlm+Onn models are calculated

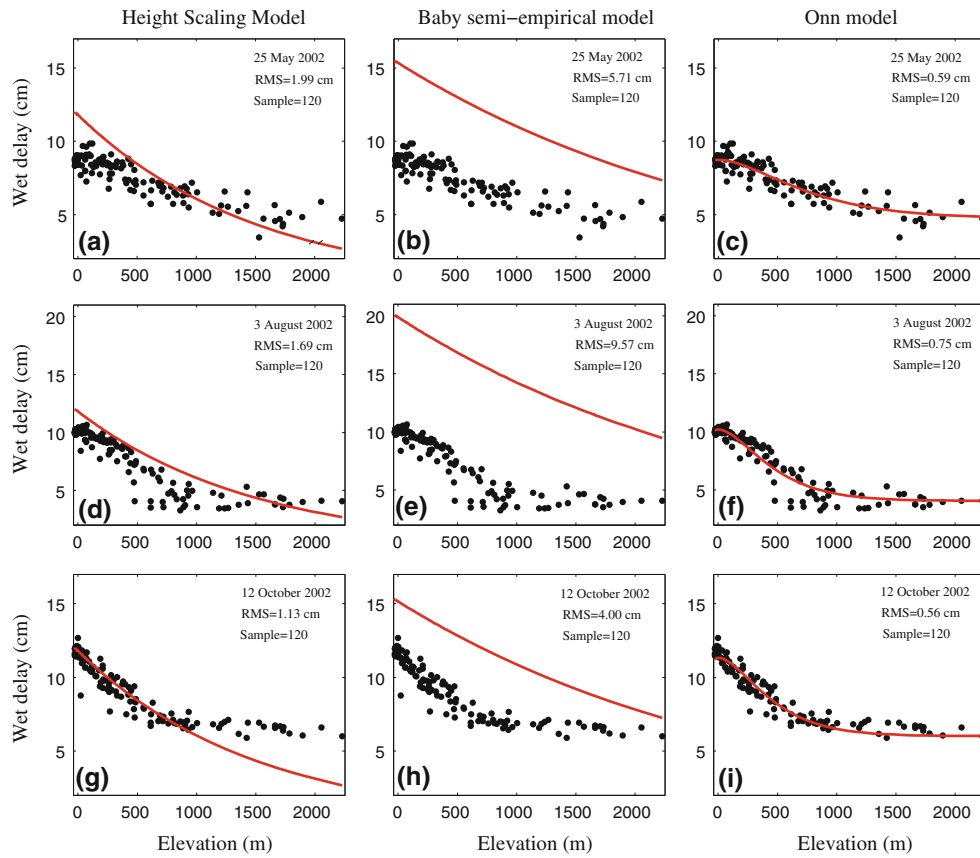


Fig. 2 GPS zenith wet delays versus elevation-dependent components of zenith wet delays calculated by different models at three chosen epochs. The *black dots* show the GPS zenith wet delays, plotted as a function of elevation. The *red solid lines* indicate the

elevation-dependent components of zenith wet delays, as scaled from the Height Scaling Model (*left column*), calculated from the Baby semi-empirical model (*middle column*), and regressed from the Onn model and available GPS zenith wet delay samples (*right column*)

based on Eq. (15) and the semivariogram model fitted in Fig. 3, while that in the BLUE+ECM model is calculated from Eqs. (5)–(7). Mean absolute error (MAE) and root mean square (RMS) between the measured zenith wet delays $Z(u_i)$ and the interpolated ones $Z^*(u_i)$ at the 20 GPS stations are used as evaluation criteria:

$$\text{MAE} = \frac{1}{20} \sum_{i=1}^{20} |[Z(u_i) - Z^*(u_i)]| \quad (17)$$

$$\text{RMS} = \sqrt{\frac{1}{20} \sum_{i=1}^{20} [Z(u_i) - Z^*(u_i)]^2}. \quad (18)$$

Figure 4 shows the differences between the measured and the interpolated zenith wet delays from the four elevation-dependent models for epoch 18:00 UTC, 25 May 2002. Also shown is the elevation of each of the GPS stations. It can be seen from the results that the trends of the zenith wet delays interpolated by the BLUE+HSM, the SKlm+Baby and the SKlm+Onn models are similar and close to the measured

values, while those by the BLUE+ECM model show significant differences. Closer examination of the results shows that the zenith wet delays interpolated by the SKlm+Onn model are on the whole closer to the values measured by GPS.

Table 1 lists the statistical results of the cross-validation analysis for the three epochs. It can be seen from the results that the SKlm+Onn interpolator has the lowest MAE and RMS errors, followed by the BLUE+HSM and the SKlm+Baby models, while the BLUE+ECM model shows the largest errors. In addition, the RMS errors of the BLUE+ECM model, ranging from 1.26 to 1.58 cm, are significantly larger than those of the other models. The reasons for the poorer performance may suggest certain deficiencies in the formulation of this model, where the elevation-dependent nature is only considered in the stochastic (covariance) model. The averaged RMS errors for the SKlm+Onn, the SKlm+Baby, the BLUE+HSM, and the BLUE+ECM models are 0.48, 0.83, 0.83, and 1.38 cm, respectively. This statistics clearly indicates that the SKlm+Onn interpolator outperforms the other models.

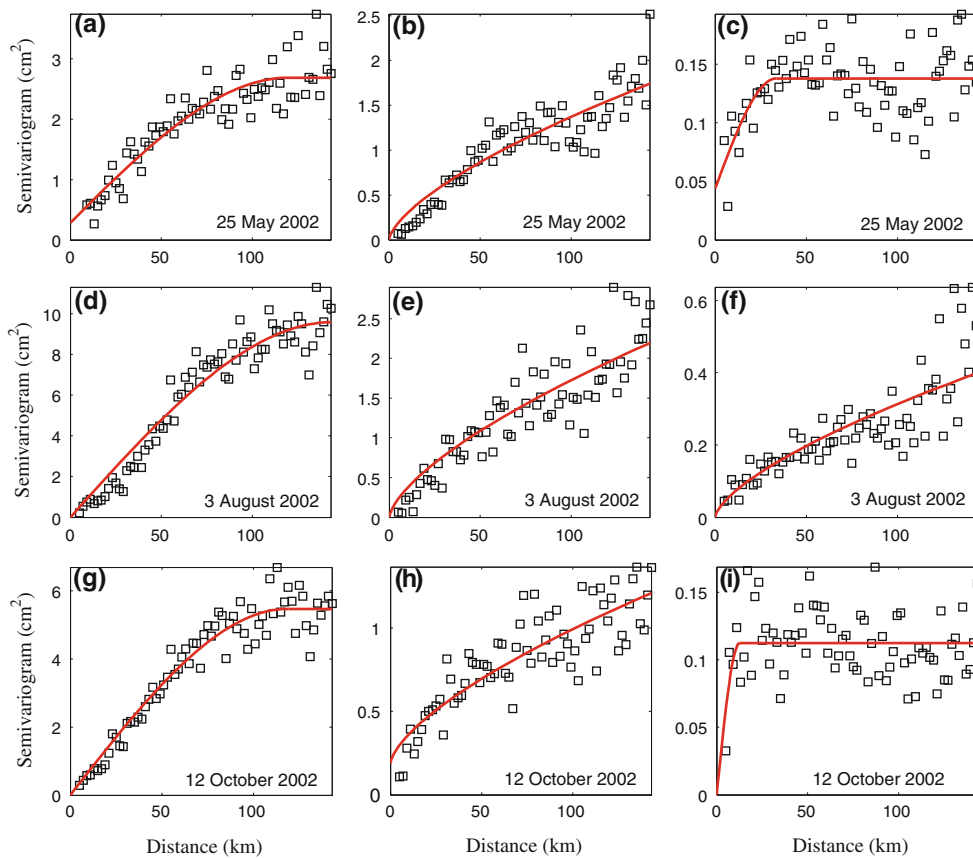


Fig. 3 Experimental semivariograms of GPS zenith wet delays (*left column*), de-trended GPS zenith wet delays (i.e., after removing the elevation-dependent components) by the Baby semi-empirical model

(*middle column*) and the Onn model (*right column*). The semivariograms in **a**, **c**, **d**, **g** and **i** follow the spherical models, while **b**, **e**, **f** and **h** follow the power law models

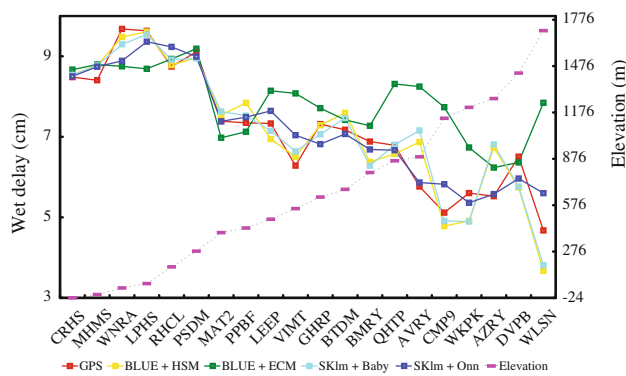


Fig. 4 Comparison between the measured and the interpolated zenith wet delays at 18:00 UTC, 25 May 2002. The *red line* shows the measured GPS zenith wet delays; the *yellow, green, light blue, and dark blue lines* denote the interpolated zenith wet delays by the BLUE + HSM, the BLUE + ECM, the SKlm + Baby and the SKlm + Onn models, respectively. Also shown are the elevations of the GPS stations (*dashed line*). The abscissa indicates the station name. The left axis of ordinates denotes the GPS zenith wet delays in cm while the right axis of ordinates denotes the elevations of GPS stations in m

Table 1 MAE and RMS differences between the measured and the interpolated zenith wet delays for the three epochs (unit: cm)

Model	25 May 2002		3 August 2002		12 October 2002	
	MAE	RMS	MAE	RMS	MAE	RMS
BLUE + HSM	0.42	0.55	0.51	0.74	0.91	1.19
BLUE + ECM	0.94	1.30	1.16	1.58	1.00	1.26
SKlm + Baby	0.43	0.57	0.68	1.00	0.68	0.92
SKlm + Onn	0.34	0.43	0.36	0.43	0.42	0.59

Although the Height Scaling Model performs better than the Baby semi-empirical model in terms of modeling the elevation-dependent component of the zenith wet delays (Fig. 2), the BLUE + HSM does not appear to be superior to the SKlm + Baby on the ground of mean *RMS* errors. This may be attributed to the fact that the deviations between the Baby semi-empirical model and the observation samples are somewhat systematic while the final interpolation accuracies

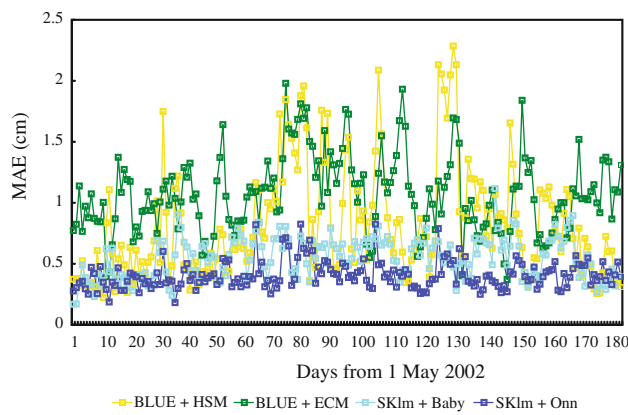


Fig. 5 Comparison of the MAE errors of the interpolations with the four interpolators. The abscissa is the number of days from 1 May 2002. The yellow, green, light blue, and dark blue lines denote the interpolation MAE errors by the BLUE + HSM, the BLUE + ECM, the SKlm + Baby, and the SKlm + Onn interpolators, respectively

are not affected too much by these deviations. Therefore, any systematic offset out of modeling the elevation-dependent component of zenith wet delay is not very critical for the interpolation. What is really important is its correlation with the height. The other contributing factor is the forms of the models, one is based on the best unbiased linear estimator and the other is on Simple Kriging (SK) to calculate the weights.

4.3 Accuracy evaluation with 6 months' zenith wet delay data

To better evaluate the accuracies of the four interpolators, we expand the above cross-validation experiment using the GPS zenith wet delay measurements at 18:00 UTC of 1 May to 31 October, 2002. The epoch is chosen because it is closest to the ERS-2 SAR acquisitions over the region as noted earlier, while the time span is chosen because the weather is hot and the water vapor motion is somewhat more active during that period. Figures 5 and 6 show the MAE and RMS differences between the measured and the interpolated zenith wet delays for dates from 1 May to 31 October, 2002. It is very obvious from these two figures that the SKlm + Onn interpolator has the lowest MAE and RMS errors, followed by the SKlm + Baby, while those of the BLUE + HSM and the BLUE + ECM are very large and with much greater variabilities.

Table 2 lists the monthly averaged MAE and RMS errors of the four interpolators. From the table, it can be seen that for all the months we studied, the MAE and RMS errors of the SKlm + Baby and the SKlm + Onn interpolators are lower than 1 cm. In comparison, the MAE and RMS errors of the BLUE + ECM interpolator are over 1 cm in nearly all months. The MAE and RMS errors of the BLUE + HSM

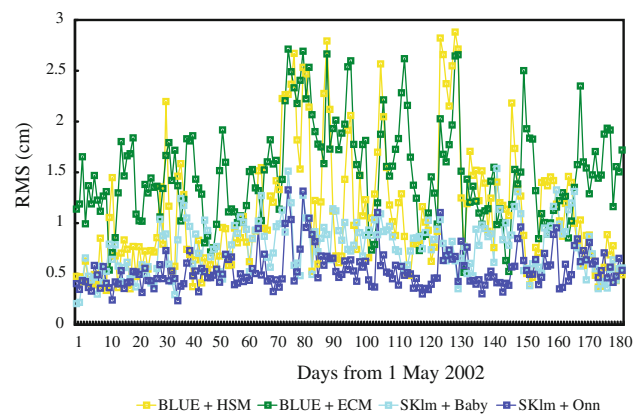


Fig. 6 Comparison of the RMS errors of the interpolations with the four interpolators. The abscissa is the number of days from 1 May 2002. The yellow, green, light blue, and dark blue lines denote the interpolation RMS errors by the BLUE + HSM, the BLUE + ECM, the SKlm + Baby, and the SKlm + Onn interpolators, respectively

interpolator are over 1 cm in nearly half of the months. For each interpolator, the greatest MAE and RMS errors appear in July consistently. Other months that also show large MAE and RMS errors are August and September. This is certainly as expected because these 3 months belong to summer season when the water vapor distribution is much more active and dynamic. The 6-month averaged RMS error for the SKlm + Onn interpolator is only 0.55 cm, while those of the SKlm + Baby, the BLUE + HSM, and the BLUE + ECM interpolators amount to 0.77, 1.11, and 1.49 cm, respectively. Thus the SKlm + Onn outperforms the other interpolators by about 29–63%.

5 Discussions and conclusions

Atmospheric water vapor delays are highly correlated with the elevation of the site. Spatial models that take the terrain elevation into account can therefore yield better results in zenith wet delays interpolation. The performance of such a model relies primarily on how accurately the elevation-dependent component of zenith wet delays is modeled. The SKlm + Baby interpolator uses the Baby semi-empirical model and the meteorological data at a reference station to model the elevation-dependent component of the zenith wet delays. The BLUE + HSM interpolator utilizes the Height Scaling Model and the zenith wet delay at a reference station. As only the observations at one reference station are used, the accuracies of the Baby semi-empirical model and the Height Scaling Model are limited (Li et al. 2006a; Elosegui et al. 1998). The elevation-dependent components of zenith wet delays can not be well modeled in these two models.

The SKlm + Onn model, however, take full advantage of the observations at all GPS stations available to determine the parameters of the Onn model, and to model the

Table 2 MAE and RMS differences between the measured and the interpolated zenith wet delays for different months (unit: cm)

Model	May		June		July		August		September		October		Average	
	MAE	RMS	MAE	RMS	MAE	RMS	MAE	RMS	MAE	RMS	MAE	RMS	MAE	RMS
BLUE+HSM	0.54	0.71	0.60	0.80	1.16	1.60	0.88	1.18	1.14	1.49	0.66	0.89	0.83	1.11
BLUE+ECM	0.92	1.28	0.99	1.31	1.37	1.95	1.11	1.53	1.02	1.43	1.01	1.40	1.07	1.49
SKIm+Baby	0.40	0.54	0.56	0.79	0.61	0.91	0.61	0.84	0.59	0.81	0.51	0.74	0.55	0.77
SKIm+Onn	0.35	0.44	0.38	0.49	0.49	0.68	0.40	0.52	0.41	0.55	0.42	0.59	0.41	0.55

elevation-dependent component of zenith wet delays. The elevation-dependent component is therefore well modeled in the SKIm+Onn model. The model is in this sense superior to the BLUE+HSM and the SKIm+Baby interpolator.

The BLUE+ECM interpolator only models the elevation dependence of zenith wet delays in the stochastic (covariance) model. This makes the zenith wet delays interpolated by the BLUE+ECM model less variable than those from the other three models, i.e., the range of the zenith wet delays being restricted, and consequently its RMS error tends to be larger and more varying.

Cross-validation analysis with GPS zenith wet delays from the SCIGN network confirms that the SKIm+Onn model outperforms the other ones compared. The 6-month averaged RMS error for the SKIm+Onn model is only 0.55 cm, while those of the SKIm+Baby, the BLUE+HSM and the BLUE+ECM models amount to 0.77, 1.11 and 1.49 cm, respectively, representing 29–63% improvement that the SKIm+Onn model is over the other ones. The SKIm+Baby and the SKIm+Onn interpolators can achieve accuracies of better than 1 cm, while the BLUE+HSM and the BLUE+ECM interpolators, in particular the BLUE+ECM interpolator, are less accurate.

In addition to InSAR water vapor correction, the proposed interpolator can also be applied to some applications within and outside geodetic fields. For example, the gridded zenith wet delays provided with the Vienna Mapping Function 1 (VMF1) can be interpolated to a GNSS site and used as a priori information in a (Kalman filter) solution based on the proposed elevation-dependent interpolator. Also at GPS and VLBI co-located sites, using the developed elevation-dependent interpolator to take into account their height difference, one common zenith wet delay can be estimated for both antennas.

It should however be noted that the SKIm+Onn interpolator requires at least three zenith wet delay samples to determine the parameters of the Onn model. More zenith wet delay samples will surely improve the determination of the Onn model and the interpolation performance of the SKIm+Onn model, but further investigations are needed. Besides, except for the accuracy of modeling the elevation-dependent component of zenith wet delays, the estimators themselves, i.e., BLUE and SK, also affect the accuracy of the zenith wet delay interpolation. This aspect is not discussed in this paper.

Acknowledgments We are grateful to Johannes Böhm and three anonymous reviewers for the constructive comments and suggestions. This work was supported by the National Natural Science Foundation of China (Nos. 40974006 and 40774003), the Research Grants Council (RGC) of the Hong Kong Special Administrative Region (Nos. PolyU5155/07E), Program for New Century Excellent Talents in Universities (NCET-08-0570), the Fundamental Research Funds for the Central Universities (No. 2009QZZD004) and the Key Laboratory for Precise Engineering Surveying & Hazard Monitoring of Hunan Province (Nos. 09K005 and 09K006).

References

- Baby HB, Gole P, Lavergnat J (1988) A model for the tropospheric excess path length of radio waves from surface meteorological measurements. *Radio Sci* 23(6):1023–1038
- Dodson AH, Shardlow PJ, Hubbard LCM, Elgered G, Jarlemark POJ (1996) Wet tropospheric effects on precise relative GPS height determination. *J Geod* 70:188–202
- Elosegui P, Rius A, Davis JL, Ruffini G, Keihm S, Burki B, Kruse LP (1998) An experiment for estimation of the spatial and temporal variations of water vapor using GPS. *Phys Chem Earth* 23(1):125–130
- Emardson TR, Elgered G, Johansson JM (1998) Three months of continuous monitoring of atmospheric water vapor with a network of Global Positioning System receivers. *J Geophys Res* 103(D2):1807–1820
- Emardson TR, Johansson JM (1998) Spatial interpolation of the atmospheric water vapor content between sites in a ground-based GPS network. *Geophys Res Lett* 25(17):3347–3350
- Emardson TR, Simons M, Webb FH (2003) Neutral atmospheric delay in interferometric synthetic aperture radar applications: Statistical description and mitigation. *J Geophys Res* 108(B5):2231. doi:[10.1029/2002JB001781](https://doi.org/10.1029/2002JB001781)
- Goovaerts P (1997) Geostatistics for natural resources evaluation. Oxford University Press, New York
- Janssen V, Ge LL, Rizos C (2004) Tropospheric correction to SAR interferometry from GPS observations. *GPS Solut* 8(3):140–151. doi:[10.1007/s10291-004-0099-1](https://doi.org/10.1007/s10291-004-0099-1)
- Jarlemark POJ, Emardson TR (1998) Strategies for spatial and temporal extrapolation and interpolation of zenith wet delay. *J Geod* 72:350–355
- Li ZW, Ding XL, Huang C, Wade G, Zheng DW (2006) Modeling of atmospheric effects on InSAR measurements by incorporating terrain elevation information. *J Atmos Solar Terres Phys* 68:1189–1194
- Li ZH, Fielding EJ, Cross P, Muller JP (2006) Interferometric synthetic aperture radar atmospheric correction: GPS topography-dependent turbulence model. *J Geophys Res* 111:B02404. doi:[10.1029/2005JB003711](https://doi.org/10.1029/2005JB003711)
- Li ZW, Ding XL, Huang C, Zou ZR, Chen YL (2007) Atmospheric effects on repeat-pass InSAR measurements over Shanghai region. *J Atmos Solar Terres Phys* 69:1344–1356
- Li ZW, Ding XL, Chen W, Liu GX, Shea YK, Emerson N (2008) Comparative study of tropospheric empirical model for Hong Kong region. *Surv Rev* 40(310):328–341
- Liu YX (2000) Remote sensing of atmospheric water vapor using GPS data in the Hong Kong region, PhD Thesis of The Hong Kong Polytechnic University, p 131
- Onn F, Zebker HA (2006) Correction for interferometric synthetic aperture radar atmospheric phase artifacts using time series of zenith wet delay observations from a GPS network. *J Geophys Res* 111:B09102. doi:[10.1029/2005JB004012](https://doi.org/10.1029/2005JB004012)
- Treuhhaft RN, Lanyi GE (1987) The effect of the dynamic wet troposphere on radio interferometric measurements. *Radio Sci* 22:251–265
- Williams S, Bock Y, Fang P (1998) Integrated satellite interferometry: Tropospheric noise, GPS estimates and implications for interferometric synthetic aperture radar products. *J Geophys Res* 103:27051–27067